

Dopamine-Triggered One-Step Polymerization and Codeposition of Acrylate Monomers for Functional Coatings

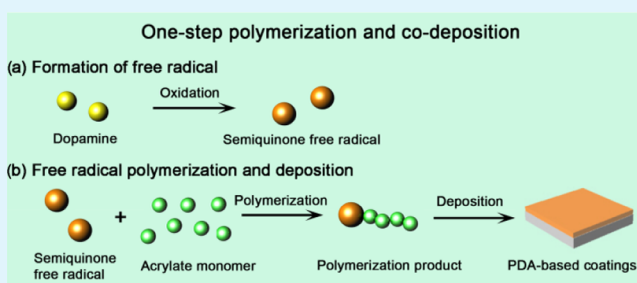
Chao Zhang,^{†,‡} Meng-Qi Ma,^{†,‡} Ting-Ting Chen,[†] He Zhang,[†] Deng-Feng Hu,[†] Bai-Heng Wu,^{†,‡} Jian Ji,[†] and Zhi-Kang Xu^{*,†,‡}

[†]MOE Key Laboratory of Macromolecular Synthesis and Functionalization, and [‡]Department of Polymer Science and Engineering, Key Laboratory of Adsorption and Separation Materials & Technologies of Zhejiang Province, Zhejiang University, Hangzhou 310027, China

Supporting Information

ABSTRACT: Surface modification has been well recognized as a promising strategy to design and exploit diversified functional materials. However, conventional modification strategies usually suffer from complicated manufacture procedures and lack of universality. Herein, a facile, robust, and versatile approach is proposed to achieve the surface functionalization using dopamine and acrylate monomers via a one-step polymerization and codeposition process. The gel permeation chromatography, proton nuclear magnetic resonance, liquid chromatography–mass spectrometry, and UV-visible spectra results indicate that dopamine possesses the capability of triggering the polymerization of acrylate monomers into high-molecular-weight products, and the inherent adhesive ability of polydopamine can assist the polymerized products to deposit on various substrates. Besides, protein-resistant, antibacterial, and cell adhesion-resistant surfaces can be easily fabricated via the finely designed integration of corresponding acrylate monomers into the codeposition systems. This approach of *in situ* polymerization and codeposition significantly simplifies the fabrication process and provides more manifold choices for surface modification, which will open a new door for broadening the applications of polydopamine-based coatings.

KEYWORDS: *mussel-inspired chemistry, dopamine-triggered polymerization, one-step method, surface functionalization, functional coating*



1. INTRODUCTION

The surface structures and properties of materials play a crucial role in their service performances in a wide range of fields, such as biomedical devices,¹ energy storage accumulators,² and environment remediation systems.³ To date, tremendous efforts have been devoted to developing different modification strategies to elaborately tune the surface structures and properties of materials,^{4–6} endowing those materials with abundant functions. However, conventional modification methods usually suffer from complex chemical/physical procedures, excessive solvent/energy consumption, or specific pretreatment for the material substrates.⁷ From a practical perspective, a desirable modification approach should possess the following features: environment-friendly process, mild reaction condition, ease of implementation, strong binding forces to the substrate surface, and versatile functionalization accessibility. Thus, it still remains a great challenge to develop an optimal modification route for tailoring and regulating the surface structures and properties of materials.

Recently, mussel-inspired polydopamine (PDA) coatings have received continually increased attention since Messersmith and co-workers reported the oxidative polymerization of dopamine and the as-formed PDA coatings on various

substrates in an alkaline medium.⁸ On the basis of the above studies, numerous dopamine derivatives with a catechol moiety have also been employed for surface modification.^{9–11} Nevertheless, unitary PDA coatings or their derivatives cannot handle various requirements because of their limited functional moieties and chemical compositions. Fortunately, one of the most celebrated features is that PDA has some unique reactive active sites to allow diversified secondary reactions.¹² For example, catechol quinone in the coatings can be nucleophilically attacked by amine- or thiol-terminated molecules. Similarly, PDA coating is able to serve as an intermediate layer for fabricating polymer brushes via initiator immobilization, followed by atom transfer radical polymerization¹³ or typical radical polymerization triggered by sunlight,¹⁴ but this approach usually calls for multiple reaction steps and harsh reaction conditions (transition-metal catalysts, light irradiation, or oxygen-free environment), immensely limiting its large-scale practical applications. Apart from the aforementioned grafting strategies, dopamine has also been introduced into the side

Received: July 27, 2017

Accepted: September 12, 2017

Published: September 12, 2017

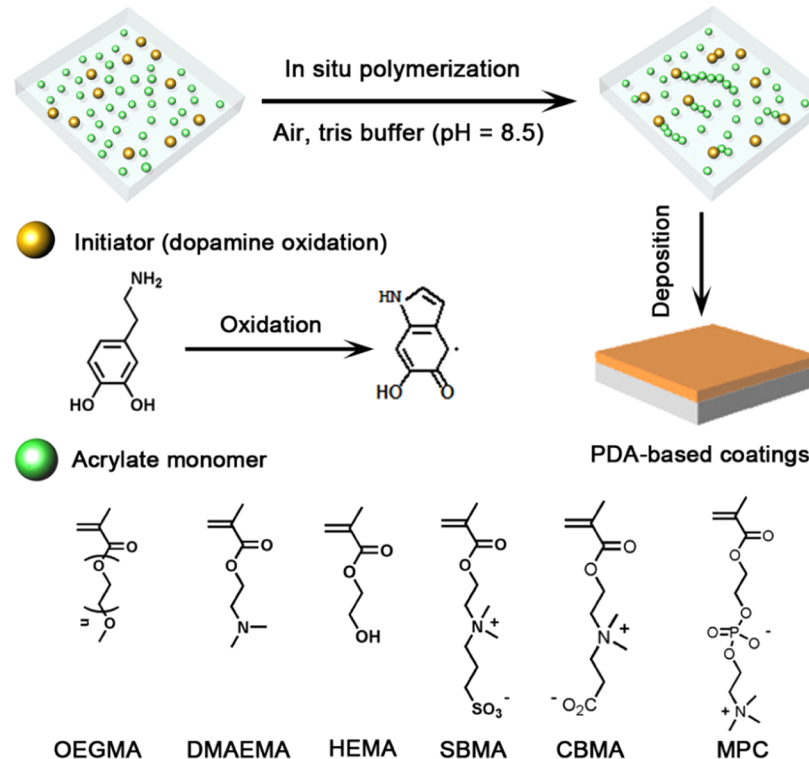


Figure 1. Schematic illustration for the fabrication process of PDA-based coatings using dopamine and acrylate monomers.

chains of some polymers, and these catechol moieties can act as adhesion sites to bind to the material surfaces for facilely obtaining functional polymer coatings.^{15,16} Although this strategy is successful in constructing multifunctional coatings, it needs to face weak adhesion forces of polymer coatings and time-consuming or cumbersome organic synthesis processes. To address these issues, we have reported a one-step codeposition route to utilize the noncovalent interactions between PDA and zwitterionic polymers for fabricating antifouling surfaces.^{17,18} Subsequently, other functional polymers were similarly used to codeposit with PDA to form a series of thin polymer films.^{19–23} However, these functional polymers require to be synthesized before codeposition, which is not a real one-step method. In addition, the codeposition strategy is not suitable for some cases in which the polymers lack interactions with PDA or shield the adhesion sites of PDA, which significantly restricts the selection range of target polymers.²⁴ Therefore, it is highly desirable to further exploit a new and universal one-step strategy to construct PDA-based functional coatings.

Although the understanding of the polymerization mechanism of dopamine still remains incomplete to date, it is well accepted that free radical species are closely connected to the polymerization of dopamine and the formation of PDA coatings.^{9,25,26} In general, dopamine is first oxidized into dopamine quinone, followed by the formation of semiquinone radical species via a single-electron exchange process and further polymerized via a radical coupling reaction.^{25,27,28} On the other hand, it is also well known that acrylate monomers are easily polymerized into polymers by typical free-radical processes.^{29,30} On the basis of these mechanisms, we propose a new one-step strategy to utilize the abundant free radicals generated during the oxidative polymerization process of dopamine to trigger the polymerization of acrylate monomers,

followed by the codeposition of the polymerized products with the assistance of PDA (Figure 1). In our cases, dopamine can directly serve as both the polymerization initiator and the surface anchoring motif, and the whole process does not require any additional catalysts or initiators. Unlike the reported codeposition based on noncovalent interactions,^{19–23} this covalent connection between the dopamine motif and the polyacrylate endows the codeposited PDA-based coatings with high stability. Besides, this route has unrivaled universality for the selectivity of both substrates and monomers, and the finely designed integration of various single or multicomponent monomers into the coatings can be used to facilely prepare protein-resistant (PDA/poly(sulfobetaine methacrylate) (PSBMA), PDA/poly(carboxybetaine methacrylate) (PCBMA), and PDA/poly(2-methacryloyloxyethyl phosphorylcholine) (PMPC) coatings), antibacterial (quaternized PDA/poly(2-(dimethylamino)ethyl methacrylate) (PDMAEMA) coatings), and cell adhesion-resistant (PDA/poly(2-hydroxyethyl methacrylate) (PHEMA) and PDA/poly[oligo(ethylene glycol)methacrylate] (POEGMA) coatings) surfaces.

2. EXPERIMENTAL SECTION

2.1. Materials. Silicon wafers were obtained from Tianjin Semiconductor Materials Institute (China). Au wafers and aluminum sheets were purchased from Alfa Aesar. Poly(ethylene terephthalate) (PET) and polyimide (PI) films were kindly provided by Hangzhou Tape Factory (China). Polypropylene microfiltration membranes (PPMMs, mean pore size ~0.2 μm) were obtained from Membrana GmbH (Germany). The silicon and Au wafers were cleaned by the piranha solution (98% H₂SO₄/30% H₂O₂, v/v = 7:3) for 20 min and rinsed with deionized water. Other substrates were washed with acetone overnight to remove impurities. Dopamine hydrochloride, iodomethane, tris(hydroxymethyl)aminomethane (Tris), sulfobetaine methacrylate (SBMA), 2-methacryloyloxyethyl phosphorylcholine (MPC), poly(ethylene glycol)methacrylate (OEGMA), 2-hydroxyethyl methacrylate (HEMA), N-isopropyl acrylamide (NIPAM), and 2-

(dimethylamino)ethyl methacrylate (DMAEMA) were purchased from Sigma-Aldrich (China), and inhibitors in all acrylate monomers were removed before use. β -Propiolactone was purchased from Macklin (China). Carboxybetaine methacrylate (CBMA) was synthesized by the reaction of DMAEMA with β -propiolactone according to previous literature.³¹ *Staphylococcus aureus* (strain American type culture collection (ATCC) 29213) and *Escherichia coli* (strain ATCC 29213) were purchased from VWR International, LLC. Fluorescein with bovine serum albumin (FL-BSA) (pI 6.0, 66.72 kDa) was purchased from Shanghai Jiahe Biotechnology Co., Ltd. (China). Smooth muscle cells (SMCs) (human umbilical artery smooth muscle cells) were purchased from ScienCell (Carlsbad, CA). Dulbecco's modified Eagle's medium (DMEM), penicillin and streptomycin, and 0.25% trypsin–ethylenediaminetetraacetic acid (EDTA) were purchased from Genom Biomedical-tech (Hangzhou, China). Fetal bovine serum (FBS) was obtained from Hyclone. Other reagents such as catechol, paraformaldehyde, sodium chloride, ethanol, hydrochloric acid, acetone, ethylether, *N,N*-dimethylformamide, and dimethyl sulfoxide were purchased from Sinopharm Chemical Reagent Co., Ltd. (China) and used without further purification. Water used in all experiments was deionized and ultrafiltrated to 18.2 M Ω cm with an ELGA Lab Water system (France).

2.2. Fabrication of Codeposited Coatings with Different Monomers. Dopamine hydrochloride and SBMA were dissolved in a Tris buffer solution ($pH = 8.5$, 50 mM). The substrates were prewetted with ethanol and then immersed in the above deposition solution, shaking for 8 h in air at 25 °C.³² Subsequently, the samples were washed with water overnight and dried with nitrogen gas or in a vacuum oven at 60 °C for 4 h before use. The concentration of dopamine was kept at 2 g/L, and the mass ratios of dopamine/SBMA were tuned from 1:0 to 1:10, 1:15, 1:25, and 1:50. Similarly, CBMA and MPC were dealt with the similar procedure, and the optimal mass ratio of dopamine/monomer was kept at 1:15.

For DMAEMA, HEMA, and OEGMA, residual inhibitors in these monomers need to be removed before use. Dopamine hydrochloride (2 g/L) was dissolved in the Tris buffer solution ($pH = 8.5$, 50 mM), and subsequently the monomer (20%, v/v) was rapidly added in the solution. Then, the substrates prewetted with ethanol were immersed in the above deposition solution, shaking for 8 h in air at 25 °C. Finally, the samples were washed with water overnight and dried with nitrogen gas or in a vacuum oven at 60 °C for 4 h before use.

2.3. Characterization. The molecular weight of the reaction product of dopamine and SBMA was characterized by gel permeation chromatography (GPC, Waters 515). The structure of the reaction product of dopamine and SBMA was confirmed by proton nuclear magnetic resonance (^1H NMR, ADVANCE DMX500; PerkinElmer) and liquid chromatography–mass spectrometry (LC–MS) (LC: Waters Crop., Milford, MA; MS: AB SCIEX, Framingham). The LC experiment used the ethylene bridged hybrid-C₁₈ column and a UV detector, and the AB TripleTOF 5600^{plus} system was applied in the MS experiment. Surface morphologies of the samples were observed using field emission scanning electron microscope (SEM) (Hitachi S4800, Japan). The surface roughness of PDA-coated silicon wafers was measured by scanning probe microscopy (multimode; Veeco). X-ray photoelectron spectra were collected by a spectrometer (X-ray photoelectron spectrometer (XPS); PerkinElmer) with Al K α excitation radiation (1486.6 eV). Fourier transform infrared (FT-IR)/attenuated total reflection (ATR) spectroscopy was conducted on an infrared spectrophotometer (Nicolet 6700) equipped with an ATR accessory (ZnSe crystal, 45°). Water contact angles were detected using a DropMeter A-200 contact angle system (MAIST Vision Inspection & Measurement Co., Ltd, China). The free radical was characterized by electron paramagnetic resonance (BRUKER A300; Brooke, Swiss). The coating thickness was detected using a spectroscopic ellipsometer (GSE-5E; Semilab Sopra, China) at an incident angel of 70°, and the light spot size was 360 × 360 μm^2 .

2.4. Antifouling Assay of PDA/PSBMA, PDA/CBMA, and PDA/PMPC Coatings. The protein resistance experiment of the samples was evaluated by static protein adsorption¹⁷ and a quartz crystal microbalance with dissipation (QCM-D) experiment con-

ducted according to a previous report. For the static protein adsorption experiment, PDA-, PDA/PSBMA-, PDA/PCBMA-, and PDA/PMPC-modified PPMMs were placed in 24-well plates and then an FL-BSA aqueous buffer solution ($pH = 7.4$, 1 mg/mL) was added into each well and incubated for 4 h at 25 °C. Subsequently, the samples were washed with ultrapure water overnight and dried in a vacuum oven at 60 °C before performing the assay. FL-BSA adsorption on the surfaces of the samples was finally detected by a fluorescence microscope (Nikon ECLIPES Ti-U, Japan), and fluorescence intensity directly displays its antifouling performance. In addition, we used QCM-D to quantificationally detect the protein adsorption. After equilibration of the baseline using a phosphate-buffered saline (PBS) solution (pH 7.4, 20 mM) at 25 °C for 1 h, the BSA solution (1 mg/mL) was flowed in the cell at a rate of 30 $\mu\text{L}/\text{min}$, finally followed by a rinse with PBS for 20 min.

2.5. Cell Adhesion Assay of PDA/PHEMA and PDA/POEGMA Coatings.

SMCs were cultured in a smooth muscle cell medium (ScienCell) in Petri dishes at 37 °C and 5% CO₂. The culture medium was changed every 3 days, and SMCs between three and eight passages at 80–90% confluence were used for initial cell adhesion experiments.

For initial cell adhesion assay, PDA-, PDA/PHEMA-, and PDA/POEGMA-modified 0.9 × 0.9 cm² silicon wafers were placed in 24-well plates and sterilized by UV for 30 min. SMCs were harvested by using trypsin–EDTA, resuspended in DMEM containing 10% FBS, and seeded onto the wafer samples at a density of 15 000 cells/cm². After a 6 h culture, the samples were washed with PBS three times, fixed with 4% paraformaldehyde in PBS, permeabilized with 0.1% Triton X-100 (Sigma), and blocked with 0.1% BSA. The samples were incubated with fluorescein isothiocyanate-labeled phalloidin (1:400; Sigma) for filamentous (F)-actin staining. Nuclei were counterstained with 4,6-diamidina-2-phenylin (Sigma). Cells were imaged with an Olympus DP72 fluorescence microscope (Olympus, Japan). The fluorescence images were analyzed with ImageJ software (v1.44p; NIH). Cell density was determined using the cell counter plugin.

2.6. Antibacterial Assay of Quaternized PDA/PDMAEMA Coatings.

First, iodomethane was dissolved in an acetone solution, and then PDA/PDMAEMA-coated silicon wafers were immersed into the mixed solution for 24 h at 25 °C. Subsequently, the samples were washed with acetone three times and blow dried with nitrogen gas before use.

Second, according to a precious antibacterial assay,³³ the nascent or quaternized PDA/PDMAEMA-coated silicon wafers were placed into a 24-well culture plate. The as-prepared bacteria were resuspended into PBS (1×10^7 cfu/mL), and 2 mL of the bacterial suspension in PBS was added onto each sample to fully cover the substrate. After 4 h at 37 °C, for the agar plate assay, 1.8 mL of PBS was added into each 24-well culture plate to dilute the bacterial solution. Then, each sample as well as the bacterial suspension was transferred to a new tube and ultrasonicated for 5 min to detach the adhered bacteria. Last, the bacterial solution was diluted to 10⁷ times, and 100 μL of the bacterial solution was taken to measure the viability of the bacteria using agar plates.

For the live/dead bacterial staining assay, the incubation of bacteria was similar to the above-mentioned procedure. Then, SYTO9 and propidium iodide were chosen to execute the staining assay, and the stained bacteria were characterized using a fluorescence microscope.

3. RESULTS AND DISCUSSION

Dopamine can easily form insoluble PDA in alkaline solutions via the oxidized polymerization and noncovalent aggregation,³⁴ causing great challenge for structure characterization. To alleviate this phenomenon, deionized water at a neutral pH value was chosen as the medium to investigate the capability of dopamine-triggered polymerization of acrylate monomers. Sulfoacetate methacrylate (SBMA) was used as a typical water-soluble monomer at first. GPC analyses show that the acrylate monomer is able to be polymerized into oligomers with a number-average molecular weight (M_n) of 3700 Da in the

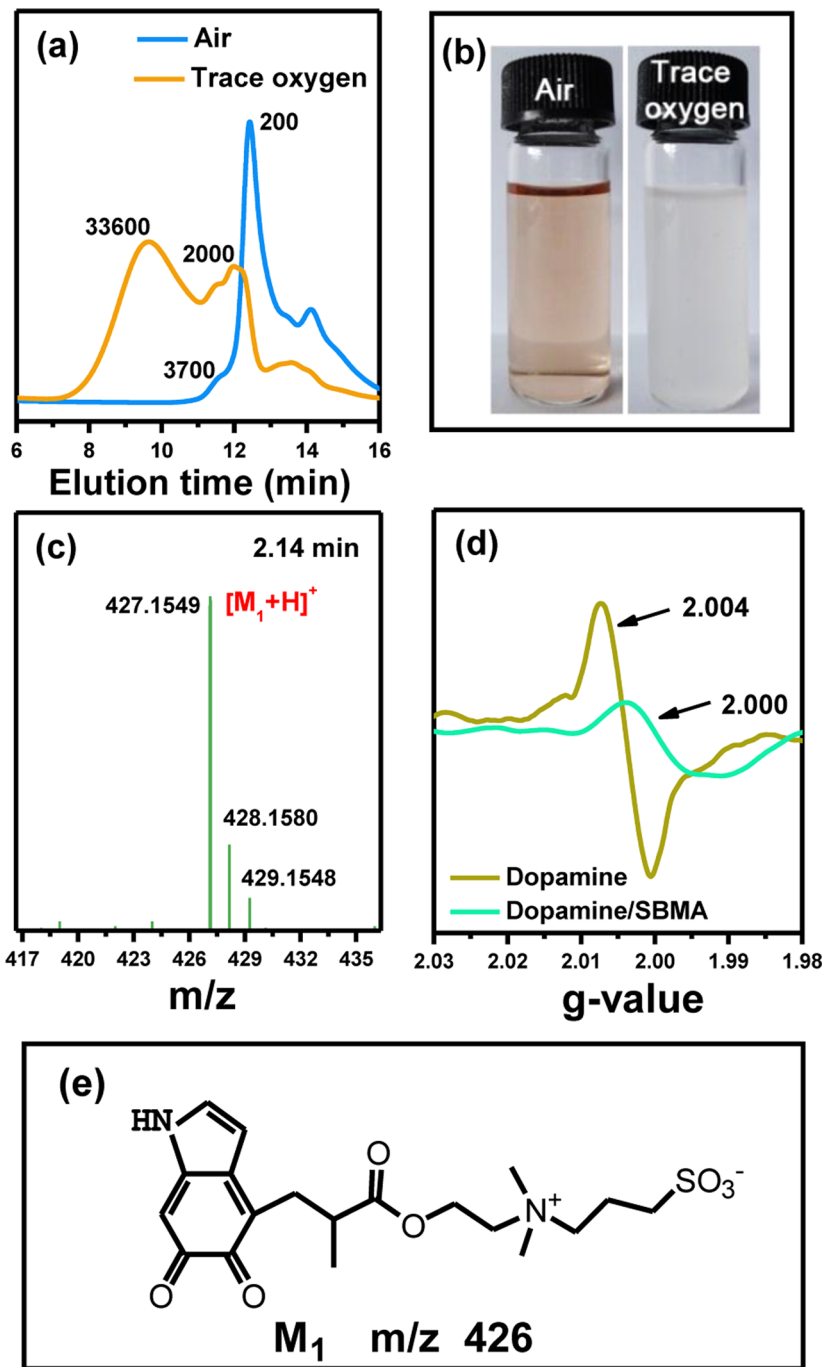
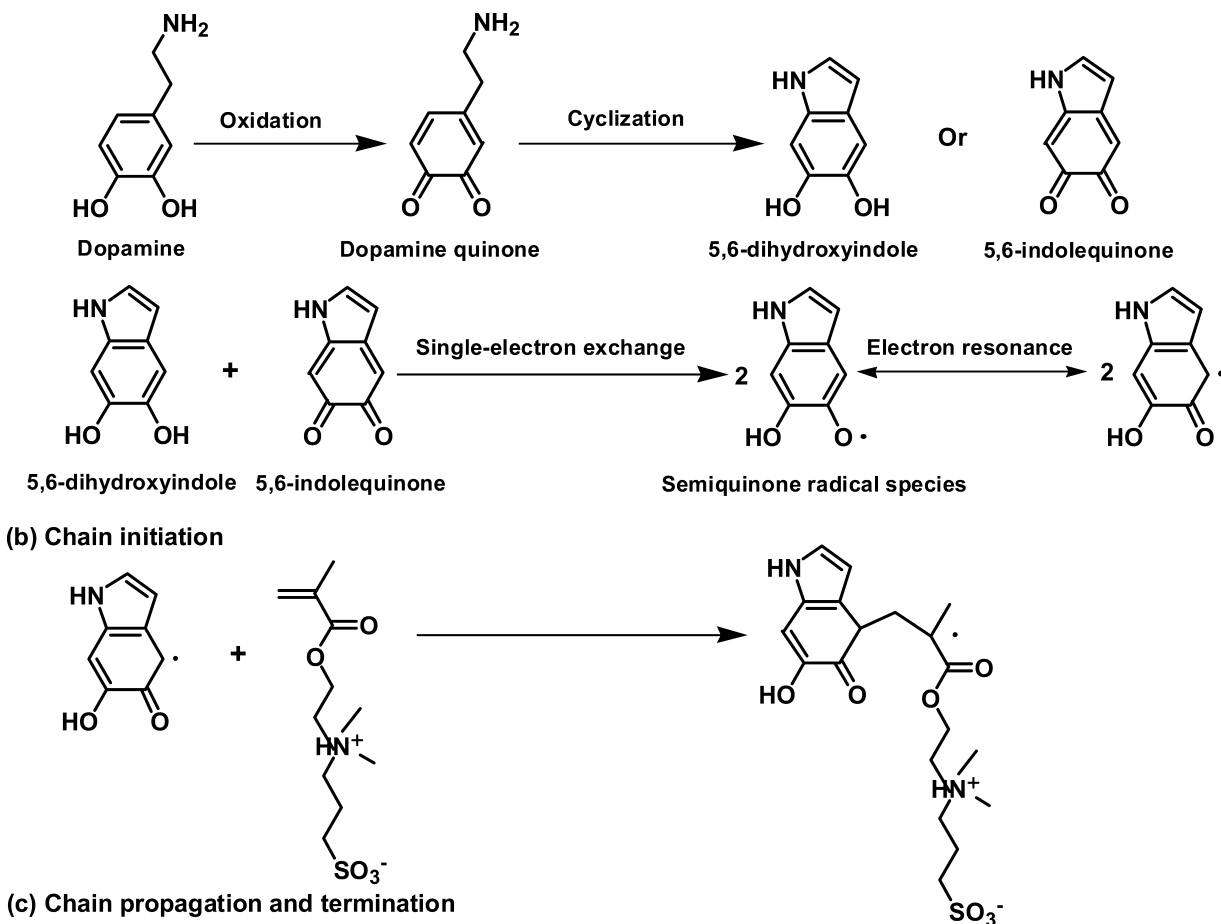


Figure 2. (a) GPC curves and (b) digital images of the mixed solutions of SBMA and dopamine after an 8 h reaction under different conditions: air and trace oxygen. The trace oxygen was achieved by bubbling N_2 to remove the majority of dissolved oxygen. (c) High-performance LC (HPLC)–MS data of the mixed solutions of SBMA and dopamine. (d) EPR curves of dopamine solutions and the mixed solutions of SBMA and dopamine. (e) Proposed molecular structure of the reaction product according to HPLC–MS analysis.

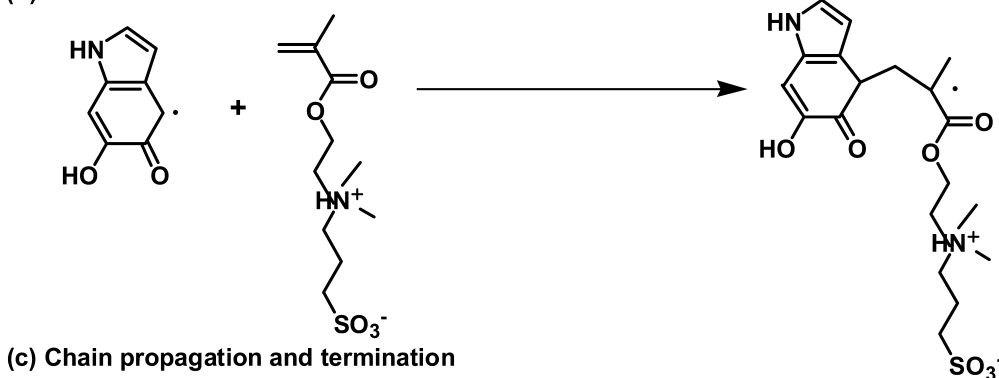
presence of dopamine in air (Figure 2a). The M_n value further increases to 33 600 Da when the majority of dissolved oxygen in the solution is removed by bubbling N_2 , and the increased rate of M_n gradually decreases as the reaction time increases (Figures 2a and S1 in Supporting Information (SI)). In addition, the polymerized products even begin to precipitate from the mixed solution after 8 h of reaction (Figure 2b). These results are consistent with the typical free-radical polymerization mechanism. In contrast, the monomer solution without dopamine has a very low M_n (~700 Da, Figure S2 in SI), indicating that the polymerization of SBMA barely happens

in the absence of a free-radical initiator. To extend the universality of our strategy, typical dopamine derivatives and acrylate monomers were employed to carry out similar experiments. Undoubtedly, catechol is also able to initiate the polymerization of SBMA, and M_n reaches 50 200 Da for the polymerized products (Figure S3 in SI). In addition, 2-hydroxyethyl methacrylate (HEMA) and N-isopropyl acrylamide (NIPAM) can be similarly polymerized with the assistance of dopamine (Figure S4 in SI). All these results demonstrate that dopamine can act as the initiator to trigger the polymerization of acrylate monomers. 1H NMR was used to

(a) Formation of radical species



(b) Chain initiation



(c) Chain propagation and termination

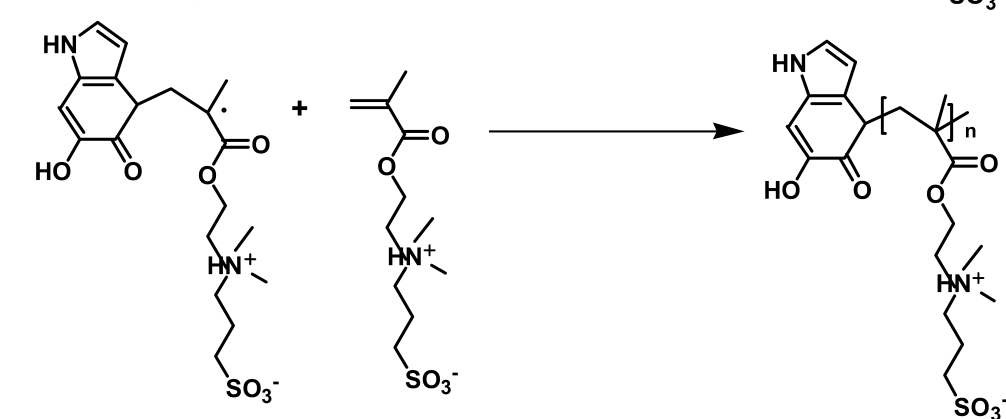


Figure 3. Suggested mechanism of the dopamine-triggered polymerization of acrylate monomers: (a) formation of radical species, (b) chain initiation, and (c) chain propagation and termination.

characterize the structures of the polymerized products of SBMA and dopamine in detail. From ^1H NMR data, the peaks at 4.45, 3.76, 3.51, 3.15, 2.93, 2.19, 1.98, and 1.05–1.29 ppm chemical shifts are all attributed to the protons of PSBMA (Figures S5 and S6 in SI). The peak at 3.65 ppm belongs to tris(hydroxymethyl)aminomethane, indicating that it can participate in the polymerization of SBMA and dopamine, which is consistent with previous results.³⁵ It is worth noting that the peaks at 6.6–7.0 ppm are ascribed to the protons from the benzene ring of dopamine, exhibiting that dopamine participates in the polymerization reaction. To further elucidate this speculation, LC–MS was utilized to analyze the connection type of dopamine and SBMA. The LC–MS data show that the

reaction product detected at the elution time of 2.14 min has a mass-to-charge ratio (m/z) of 427 (Figures S7, SI and 2c), which corresponds to the protonated product ($[\text{M}_1 + \text{H}]^+$) (Figure 2e). This illustrates that SBMA is linked to the benzene ring of dopamine by a covalent bond. In addition, the solution color of PSBMA initiated via dopamine oxidation turns yellow after the addition of $\text{K}_2\text{S}_2\text{O}_8$, and its UV–visible (vis) absorbance is much higher than that of PSBMA synthesized by typical free-radical polymerization (Figure S8 in SI). These behaviors further demonstrate that the polymerized products contain some dopamine motifs, and the connection type is a covalent bond because all polymerized products were dialyzed against ultrapure water for 3 days to completely remove

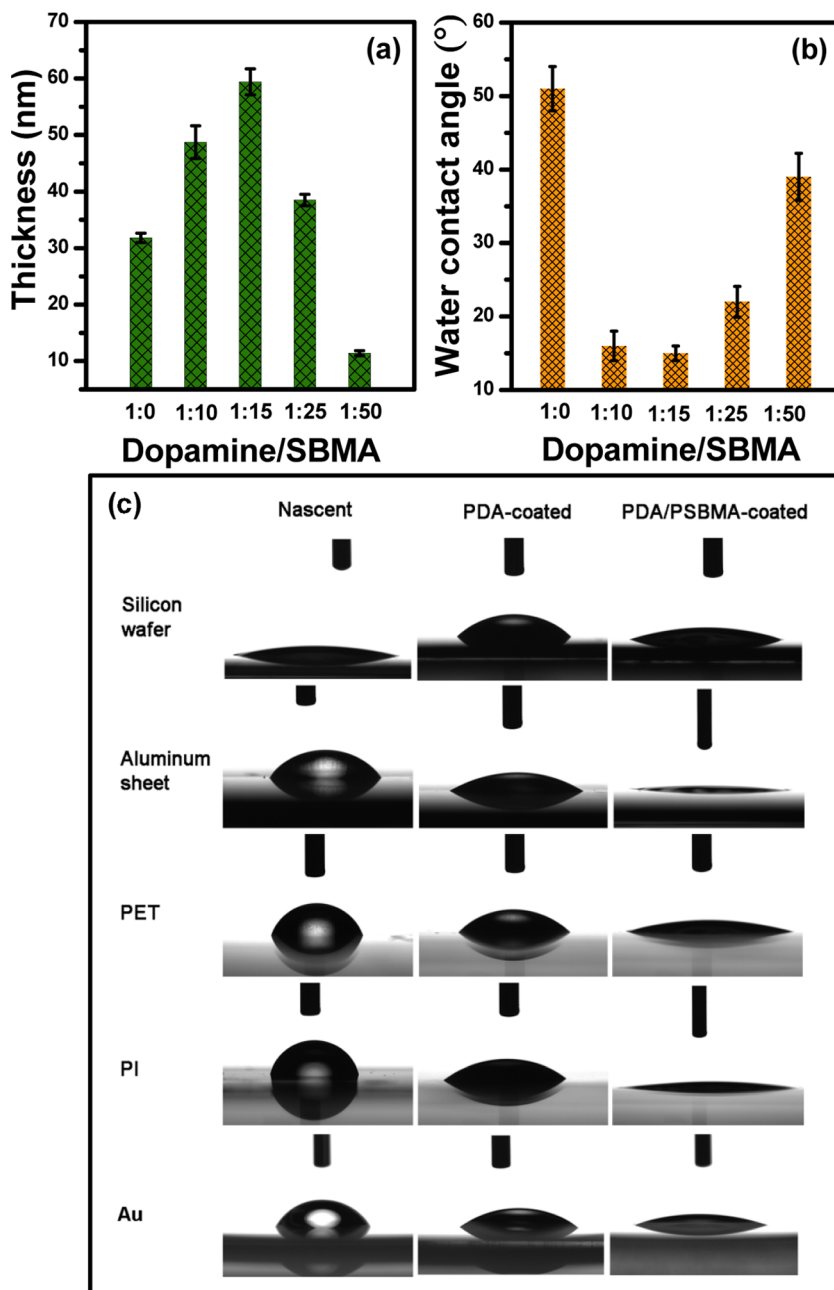


Figure 4. (a) Thickness and (b) water contact angle of PDA/PSBMA coatings on silicon wafers with dopamine/SBMA mass ratios of 1:0, 1:10, 1:15, 1:25, and 1:50, respectively. (c) Water contact images of nascent, PDA, and PDA/PSBMA coatings on different substrates. The dopamine/SBMA mass ratio is 1:15. The deposition time is 8 h. PET: poly(ethylene terephthalate) and PI: polyimide.

residual monomers and initiators. In combination with the results of GPC, ¹H NMR, LC–MS, and UV–vis spectra, dopamine exhibits the capability of serving as an initiator to trigger the polymerization of acrylate monomers.

To reliably reveal the polymerization mechanism in our cases, EPR was employed to characterize the free radicals during the reaction process. In view of only dopamine, the *g*-value is around 2.004 (Figure 2d), which corresponds to a typical melanin semiquinone free radical.³⁶ By contrast, the *g*-value reduces to 2.000 after the addition of SBMA. It demonstrates that the semiquinone free radical transfers to the acrylate monomer via chain initiation (Figure 3b). Therefore, we propose a reasonable mechanism for the dopamine-triggered polymerization of acrylate monomers on

the basis of the above-mentioned results and the reported oxidation polymerization of dopamine (Figure 3a–c). In an alkaline condition, dopamine is first oxidized into dopamine quinone, followed by the formation of 5,6-dihydroxyindole via intramolecular cyclization. 5,6-Dihydroxyindole is further oxidized into 5,6-indolequinone. Subsequently, both 5,6-dihydroxyindole and 5,6-indolequinone transfer into semiquinone radical species via the single-electron exchange reaction, which further forms relatively stable free radicals by the electron resonance. These radicals can integrate into dimers or trimers via the radical coupling reaction, which is the typical route for the oxidation polymerization of dopamine.^{37,38} In our cases, they can not only proceed with the coupling reaction,

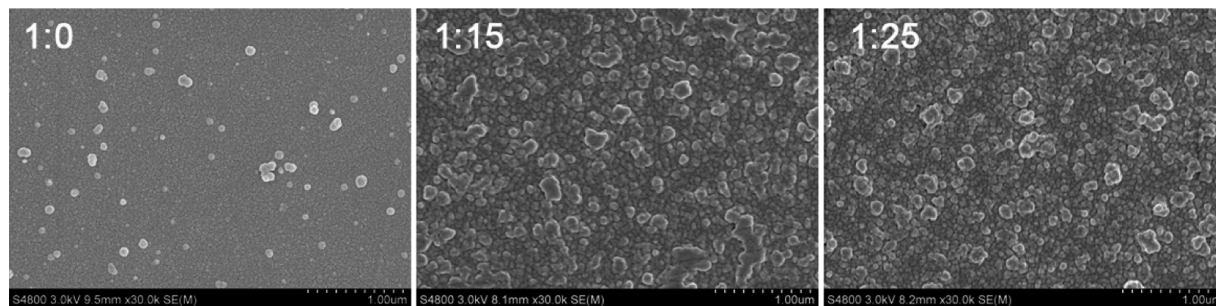


Figure 5. SEM images of PDA/PSBMA coatings on silicon wafers with different dopamine/SBMA mass ratios (1:0, 1:15, and 1:25). The deposition time is 8 h.

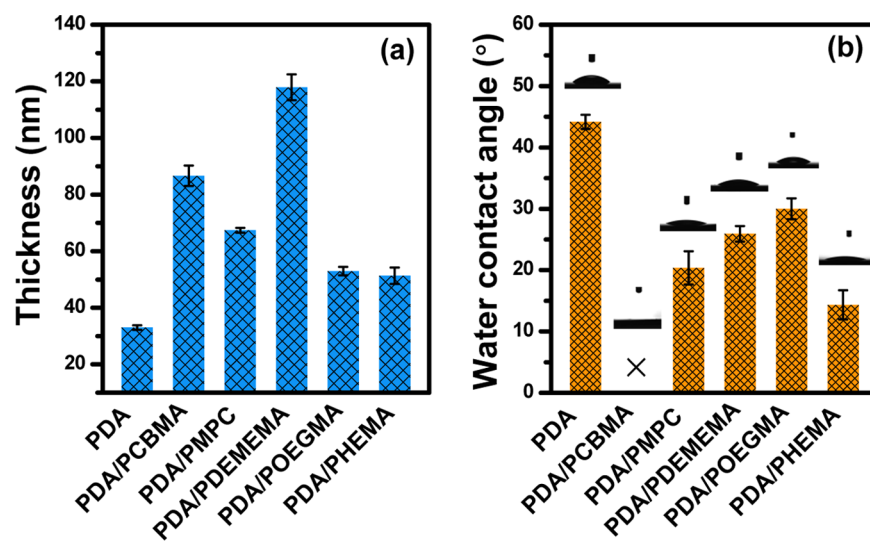


Figure 6. (a) Thickness, (b) water contact angle, and corresponding images of the codeposited coatings on silicon wafers via deposition of dopamine and different acrylate monomers. The deposition time is 8 h. “X” Indicates that the water drop spreads fast on the surface, and the water contact angle is nearly 0°.

but also act as reactive species to initiate the free-radical polymerization of acrylate monomers to form polymers.

It is reasonable to expect that the acrylate monomers will influence the aggregation and deposition of the polymerized products. It can be seen that numerous PDA aggregations precipitate from the dopamine solution after the 8 h reaction. However, this phenomenon does not happen when SBMA is added into the dopamine solution (Figure S9 in SI). Furthermore, the solution color gradually turns pale with the increase in the SBMA concentration. It should be noted that the solution remains transparent for 1 month when the mass ratio of dopamine/SBMA is 1:50 or even lower. This means excess SBMA will efficiently inhibit the aggregation of the polymerized products because the hydrophilicity of aggregations is enhanced by the chemically bonded SBMA units. Figure 4a shows that the coating thickness first increases and then decreases along with the increase in the SBMA concentration. It reaches 59.4 ± 2.3 nm after 8 h of deposition when the mass ratio of dopamine/SBMA is 1:15, which is twice as high as that of PDA deposition without SBMA (31.8 ± 0.84 nm). In contrast, the coating thickness is only 11.4 ± 0.5 nm when the mass ratio of dopamine/SBMA is 1:50, resulting from the fact that its aggregations are relatively stable in the deposition solution (Figure S9 in SI) to lead to a low deposition thickness. The chemical structures of the coatings were analyzed by XPS and FT-IR/ATR (Figure S10 and Table

S1 in SI). Compared with the XPS spectrum of PDA coating, a new peak for S2p3 appears. Similarly, the FT-IR/ATR spectra have some new peaks at 1729 and 1042 cm^{-1} that are attributed to the O=C=O stretching vibration and the S=O symmetric stretching vibration, respectively, due to the incorporation of SBMA units. In addition, the intensity of characteristic peaks gradually increases along with the increase in the deposition time (Figure S11 in SI). The surface morphologies of PDA/PSBMA coatings were surveyed by SEM and atomic force microscopy (AFM). It is obvious that these coatings contain relatively larger nanoparticles (70.39 ± 10.39 nm) than that of PDA coating (42.36 ± 5.88 nm), and their surface roughness increases from 1.9 to 5.8 nm due to the introduction of SBMA units (Figures 5 and S12 in SI). A possible reason for these large particles and the surface roughness is that the PDA/PSBMA nanoaggregates need to grow into relatively large particles to possess enough adhesive sites for depositing on the substrate surface. It should be pointed out that the incorporation of PSBMA will decrease the adhesive force of PDA/PSBMA aggregates because of the reduction of adhesive dopamine sites.³⁹ The surface wettability was characterized by measuring the water contact angle (WCA) on the coatings. Figure 4b shows that the WCA declines to $<20^\circ$ when the mass ratio of dopamine/SBMA is 1:10 and 1:15 for fabricating the coatings, which is ascribed to the intrinsic hydrophilicity of PSBMA. The changes of WCA were also employed to assess

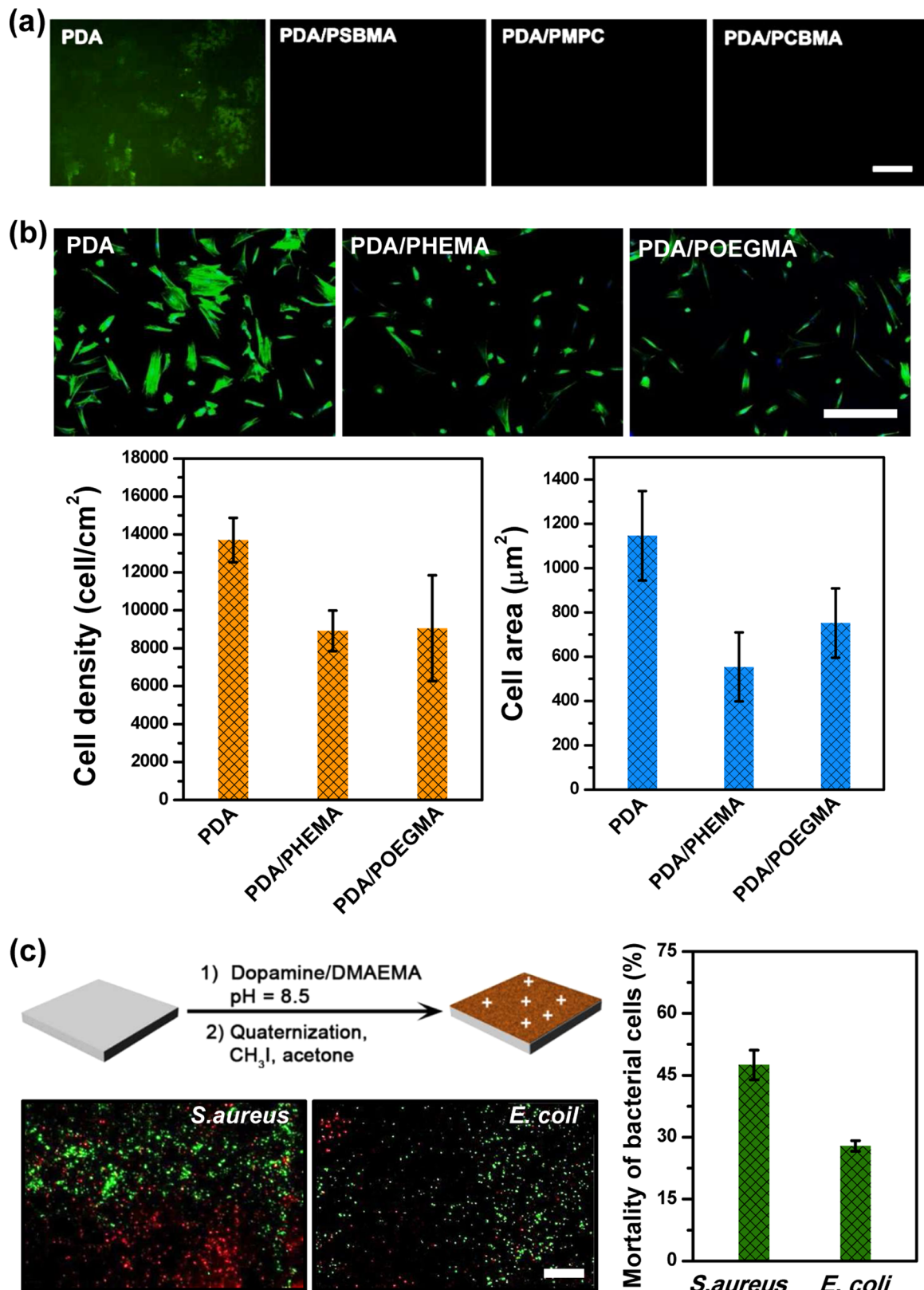


Figure 7. (a) Fluorescence microscopy images of FL-BSA adsorption on the PDA-, PDA/PSBMA-, PDA/PCBMA-, and PDA/PMPC-coated surfaces. The scale bar is 100 μm . (b) Fluorescence microscopy images of cell adhesion, cell density, and cell area on the PDA-, PDA/PHEMA-, and PDA/POEGMA-coated surfaces. Human umbilical cord smooth muscle cells were used as model cells. F-actin was stained green. Nuclei were stained blue. The scale bar represents 200 μm . (c) Antibacterial performances of PDA/PDMAEMA-coated surfaces after quaternization treatment. Green and red fluorescence represents live and dead bacteria, respectively. The scale bar is 100 μm .

the structural stability of coatings after different treatments (Figure S13 in SI). It is noted that the WCA of the PDA/PSBMA coatings has almost no change and still remains $<20^\circ$ after treated by 0.1 M NaCl, ethanol, acetone, acid solution ($\text{pH} \geq 3$), and alkaline solution ($\text{pH} \leq 11$). In addition, the retention ratio of the coating thickness is almost 90% after 72 h of treatment in the presence of the above-mentioned solvents (Figure S14 in SI). All these results indicate that the dopamine-triggered covalent connections bestow the coatings with excellent stability and durability. Furthermore, the PDA/PSBMA coatings appear almost colorless (Figure S15 in SI), which overcomes another disadvantage for PDA-based coatings with brown to dark coloration.⁴⁰ The transmittance of glass at 400 nm decreases slightly from 90 to 80% after the codeposition of PDA/PSBMA coatings (Figure S15 in SI). In contrast, it declines to 55% when coated by PDA.

Different substrates and acrylate monomers were further investigated to assess the universality of the dopamine-triggered one-step polymerization and deposition. Figure 4c demonstrates that PDA/PSBMA coatings can be facilely constructed on an alumina sheet, polyimide (PI) film, and Au wafer, apart from the aforementioned silicon wafer, glass wafer, and poly(ethylene terephthalate) (PET) film. This implies that our strategy still maintains excellent material-independent properties as PDA can form multiple noncovalent interactions with these above-mentioned substrates, such as hydrogen bonding, coordination interaction, cation– π interaction, π – π stacking, and hydrophobic interaction.³ Furthermore, this strategy is extensively suitable for a series of water-soluble acrylate monomers, including 2-methacryloxyethyl phosphorylcholine (MPC), carboxybetaine methacrylate (CBMA), poly(ethylene glycol) methacrylate (OEGMA), 2-hydroxyethyl methacrylate (HEMA), and 2-(dimethylamino)ethyl methacrylate (DMAEMA). Figure 6 indicates that the addition of these acrylate monomers results in increases in both the coating thickness and the surface hydrophilicity. FT-IR/ATR spectra of the coatings show characteristic peaks from the functional groups of the corresponding polymers (Figure S16 in SI). The O/C ratio of the coating surfaces is much higher than that of pure PDA (Table S2 in SI). In addition, the acrylate monomers have a significant influence on the surface morphology of the PDA-based coatings (Figure S17 in SI). The possible reason is that PDA aggregates modified by different polymers immensely affect the interactions among them, which in turn leads to the size and morphology changes of the aggregates. All these results indicate that various coatings can be facilely constructed by the dopamine-triggered one-step polymerization and deposition strategy. It is worth noting that some polymers have very weak interactions with PDA or can shield the adhesion sites of PDA aggregates, leading to the poor codeposition efficiency. For example, the interactions between poly(ethylene glycol) and PDA are only weak hydrogen bonds, and their codeposition is very inefficient or even difficult to realize.²⁴ Fortunately, our strategy can overcome these disadvantages and exploit a new insight to realize the covalent connection between dopamine and OEGMA, followed by the codeposition for fabricating PDA/POEGMA coatings. Another issue is that apart from the single acrylate monomer, our approach can similarly utilize multicomponents to construct composite PDA-based coatings. For example, PDA/PSBMA/PMPC coatings are easily fabricated by the dopamine-triggered one-step copolymerization and codeposition of SBMA and MPC (Table S3 in SI).

Therefore, diversified acrylate monomers are able to be integrated into the one-step polymerization and codeposition system, providing tremendous opportunities to develop diversified functional coatings for different applications. For example, we can utilize zwitterionic monomers to fabricate protein resistance coatings because PSBMA, PCBMA, and PMPC have been well recognized as excellent antifouling materials.⁴¹ Figure 7a shows the fluorescence microscopy images of FL-BSA adsorption on the coating surfaces fabricated by our strategy. It can be seen that the PDA/PSBMA, PDA/PMPC, and PDA/PCBMA coatings have almost undetectable fluorescence, whereas PDA still displays strong fluorescence. In addition, QCM-D results show that the protein adsorption of the PDA/PSBMA-coated gold sensor is only 19.17 ng/cm², which is much lower than that of the nascent gold sensor (252.52 ng/cm²) and PDA-coated gold sensor (62.00 ng/cm²) (Figure S18 in SI). All these results indicate that the introduction of zwitterionic polymers endows the coatings with outstanding performance of resistance to protein adsorption. Another example is that the PDA/PHEMA and PDA/POEGMA coatings are facilely fabricated with good biocompatibility to reduce cell adhesion.^{42–44} Figure 7b shows that most of the vascular smooth muscle cells (SMCs) on the PDA coatings have a well-spread morphology. However, the PDA/PHEMA and PDA/POEGMA coatings significantly reduce the adhesion of SMCs. Besides, the fluorescence images similarly show that many SMCs display a round and poorly spread morphology on these coating surfaces. Both the cell density and the cell area indicate that the PDA/PHEMA and PDA/POEGMA coatings are able to significantly inhibit cell adhesion compared to that of the PDA ones. These results suggest that our coatings have great potential as a surface modification strategy for cardiovascular implants to reduce the hyperplasia of SMCs and to inhibit the in-stent restenosis. Furthermore, our strategy has also been adopted to construct antibacterial surfaces with quaternized polymers.¹⁵ In these cases, DMAEMA and dopamine were mixed to fabricate PDA/PDMAEMA coatings, followed by quaternization treatment for the antibacterial surfaces. *S. aureus* and *E. coli* were chosen to evaluate the antibacterial performance of the as-prepared coatings. It can be seen that the quaternized PDA/PDMAEMA coatings are able to kill many bacteria, especially *S. aureus*, in the live/dead bacteria assay (Figures 7c and S19 in SI). The sterilization efficiency is 45.7 and 27.8% for *S. aureus* and *E. coli*, respectively. Although this efficiency is relatively moderate, it also indicates that our strategy is valid for fabricating PDA-based coatings. Overall, functional coatings can be facilely constructed by introducing various acrylate monomers into the dopamine-triggered one-step polymerization and codeposition strategy.

4. CONCLUSIONS

In summary, we report a strategy to use dopamine-triggered one-step polymerization and deposition of acrylate monomers for surface modification. This is the first report to propose dopamine as the polymerization initiator and to realize the codeposition of PDA and as-formed polymers at the same time. The greatest advantage of this strategy is the excellent universality, such as material-independent properties and diversification of available monomers. Besides, various functional coatings can be facilely constructed by the introduction of different monomers. Moreover, the color of codeposited coatings is much lighter compared to that of pure PDA

coatings. To the best of our knowledge, this is the simplest method for fabricating PDA-based functional coatings up to now, which provides new insight into the development of mussel-inspired chemistries and materials.

■ ASSOCIATED CONTENT

Supporting Information

The Supporting Information is available free of charge on the ACS Publications website at DOI: [10.1021/acsami.7b11092](https://doi.org/10.1021/acsami.7b11092).

Number-average molecular weight (M_n) of the polymerized products under different reaction time points; GPC curves of the mixed solutions of catechol/SBMA and dopamine/typical acrylate monomers; ^1H NMR curve of the reaction product of dopamine and SBMA; digital images of the mixed solutions of dopamine/SBMA; XPS and FT-IR/ATR spectra of different PDA-based coatings; SEM and AFM images of different PDA-based coatings; water contact angles and transmittance of PDA/PSBMA coatings; protein adsorption ability measured by QCM-D; digital images and UV-vis spectra of PSBMA solutions; fluorescence microscopy images of a live/dead assay on the nascent silicon wafer ([PDF](#))

■ AUTHOR INFORMATION

Corresponding Author

*E-mail: xuzk@zju.edu.cn.

ORCID

Jian Ji: [0000-0001-9870-4038](https://orcid.org/0000-0001-9870-4038)

Zhi-Kang Xu: [0000-0002-2261-7162](https://orcid.org/0000-0002-2261-7162)

Notes

The authors declare no competing financial interest.

■ ACKNOWLEDGMENTS

The authors acknowledge the financial support by the National Natural Science Foundation of China (Grant no. 21534009).

■ REFERENCES

- (1) Ku, S. H.; Ryu, J.; Hong, S. K.; Lee, H.; Park, C. B. General Functionalization Route for Cell Adhesion on Non-wetting Surfaces. *Biomaterials* **2010**, *31*, 2535–2541.
- (2) Zhou, W.; Xiao, X.; Cai, M.; Yang, L. Polydopamine-coated, Nitrogen-doped, Hollow Carbon–sulfur Double-layered Core–shell Structure for Improving Lithium–sulfur Batteries. *Nano Lett.* **2014**, *14*, 5250–5256.
- (3) Yang, H.-C.; Luo, J.; Lv, Y.; Shen, P.; Xu, Z.-K. Surface Engineering of Polymer Membranes via Mussel-inspired Chemistry. *J. Membr. Sci.* **2015**, *483*, 42–59.
- (4) Sedó, J.; Saiz-Poseu, J.; Busqué, F.; Ruiz-Molina, D. Catechol-Based Biomimetic Functional Materials. *Adv. Mater.* **2013**, *25*, 653–701.
- (5) Ryu, D. Y.; Shin, K.; Drockenmuller, E.; Hawker, C. J.; Russell, T. P. A Generalized Approach to the Modification of Solid Surfaces. *Science* **2005**, *308*, 236–239.
- (6) Borges, J.; Mano, J. F. Molecular Interactions Driving the Layer-by-Layer Assembly of Multilayers. *Chem. Rev.* **2014**, *114*, 8883–8942.
- (7) Wei, Q.; Haag, R. Universal Polymer Coatings and Their Representative Biomedical Applications. *Mater. Horiz.* **2015**, *2*, 567–577.
- (8) Lee, H.; Dellatore, S. M.; Miller, W. M.; Messersmith, P. B. Mussel-inspired Surface Chemistry for Multifunctional Coatings. *Science* **2007**, *318*, 426–430.
- (9) Liu, Y.; Ai, K.; Lu, L. Polydopamine and Its Derivative Materials: Synthesis and Promising Applications in Energy, Environmental, and Biomedical Fields. *Chem. Rev.* **2014**, *114*, 5057–5115.
- (10) Ye, Q.; Zhou, F.; Liu, W. Bioinspired Catecholic Chemistry for Surface Modification. *Chem. Soc. Rev.* **2011**, *40*, 4244–4258.
- (11) Hong, S.; Kim, J.; Na, Y. S.; Park, J.; Kim, S.; Singha, K.; Im, G.-I.; Han, D.-K.; Kim, W. J.; Lee, H. Poly(norepinephrine): Ultrasmooth Material-independent Surface Chemistry and Nanodepot for Nitric Oxide. *Angew. Chem., Int. Ed.* **2013**, *52*, 9187–9191.
- (12) Lee, H.; Rho, J.; Messersmith, P. B. Facile Conjugation of Biomolecules onto Surfaces via Mussel Adhesive Protein Inspired Coatings. *Adv. Mater.* **2009**, *21*, 431–434.
- (13) Li, C. Y.; Wang, W. C.; Xu, F. J.; Zhang, L. Q.; Yang, W. T. Preparation of pH-sensitive Membranes via Dopamine-initiated Atom Transfer Radical Polymerization. *J. Membr. Sci.* **2011**, *367*, 7–13.
- (14) Sheng, W.; Li, B.; Wang, X.; Dai, B.; Yu, B.; Jia, X.; Zhou, F. Brushing up from “Anywhere” under Sunlight: A Universal Surface-initiated Polymerization from Polydopamine-coated Surfaces. *Chem. Sci.* **2015**, *6*, 2068–2073.
- (15) Yang, C.; Ding, X.; Ono, R. J.; Lee, H.; Hsu, L. Y.; Tong, Y. W.; Hedrick, J.; Yang, Y. Y. Brush-like Polycarbonates Containing Dopamine, Cations, and PEG Providing a Broad-spectrum, Antibacterial, and Antifouling Surface via One-step Coating. *Adv. Mater.* **2014**, *26*, 7346–7351.
- (16) Li, L.; Yan, B.; Zhang, L.; Tian, Y.; Zeng, H. Mussel-inspired Antifouling Coatings Bearing Polymer Loops. *Chem. Commun.* **2015**, *51*, 15780–15783.
- (17) Zhou, R.; Ren, P.-F.; Yang, H.-C.; Xu, Z.-K. Fabrication of Antifouling Membrane Surface by Poly(sulfobetaine methacrylate)/Polydopamine Co-deposition. *J. Membr. Sci.* **2014**, *466*, 18–25.
- (18) Zhang, C.; Li, H.-N.; Du, Y.; Ma, M.-Q.; Xu, Z.-K. CuSO₄/H₂O₂-Triggered Polydopamine/Poly(sulfobetaine methacrylate) Coatings for Antifouling Membrane Surfaces. *Langmuir* **2017**, *33*, 1210–1216.
- (19) Chang, C.-C.; Kolewe, K. W.; Li, Y.; Kosif, I.; Freeman, B. D.; Carter, K. R.; Schiffman, J. D.; Emrick, T. Underwater Superoleophobic Surfaces Prepared from Polymer Zwitterion/Dopamine Composite Coatings. *Adv. Mater. Interfaces* **2016**, *3*, No. 1500521.
- (20) Wang, Z.-X.; Lau, C.-H.; Zhang, N.-Q.; Bai, Y.-P.; Shao, L. Mussel-inspired Tailoring of Membrane Wettability for Harsh Water Treatment. *J. Mater. Chem. A* **2015**, *3*, 2650–2657.
- (21) Xu, Y. C.; Tang, Y. P.; Liu, L. F.; Guo, Z. H.; Shao, L. Nanocomposite Organic Solvent Nanofiltration Membranes by a Highly-efficient Mussel-inspired Co-deposition Strategy. *J. Membr. Sci.* **2017**, *526*, 32–42.
- (22) Kirschner, A. Y.; Chang, C.-C.; Kasemset, S.; Emrick, T.; Freeman, B. D. Fouling-resistant Ultrafiltration Membranes Prepared via Co-deposition of Dopamine/Zwitterion Composite Coatings. *J. Membr. Sci.* **2017**, *541*, 300–311.
- (23) Kolewe, K. W.; Dobosz, K. M.; Rieger, K. A.; Chang, C.-C.; Emrick, T.; Schiffman, J. D. Antifouling Electrospun Nanofiber Mats Functionalized with Polymer Zwitterions. *ACS Appl. Mater. Interfaces* **2016**, *8*, 27585–27593.
- (24) Zhang, Y.; Thingholm, B.; Goldie, K. N.; Ogaki, R.; Städler, B. Assembly of Poly(dopamine) Films Mixed with a Nonionic Polymer. *Langmuir* **2012**, *28*, 17585–17592.
- (25) Du, X.; Li, L.; Li, J.; Yang, C.; Frenkel, N.; Welle, A.; Heissler, S.; Nefedov, A.; Grunze, M.; Levkin, P. A. UV-triggered Dopamine Polymerization: Control of Polymerization, Surface Coating, and Photopatterning. *Adv. Mater.* **2014**, *26*, 8029–8033.
- (26) Riley, P. A. Radicals in Melanin Biochemistry. *Ann. N. Y. Acad. Sci.* **1988**, *551*, 111–119.
- (27) Zhang, C.; Ou, Y.; Lei, W.-X.; Wan, L.-S.; Ji, J.; Xu, Z.-K. CuSO₄/H₂O₂-induced Rapid Deposition of Polydopamine Coatings with High Uniformity and Enhanced Stability. *Angew. Chem., Int. Ed.* **2016**, *55*, 3054–3057.
- (28) Zhang, C.; Lv, Y.; Qiu, W.-Z.; He, A.; Xu, Z.-K. Polydopamine Coatings with Nanopores for Versatile Molecular Separation. *ACS Appl. Mater. Interfaces* **2017**, *9*, 14437–14444.
- (29) Anseth, K. S.; Wang, C. M.; Bowman, C. N. Kinetic Evidence of Reaction Diffusion during the Polymerization of Multi (meth) Acrylate Monomers. *Macromolecules* **1994**, *27*, 650–655.

- (30) Jansen, J. F. G. A.; Dias, A. A.; Dorschu, M.; Coussens, B. Fast Monomers: Factors Affecting the Inherent Reactivity of Acrylate Monomers in Photoinitiated Acrylate Polymerization. *Macromolecules* **2003**, *36*, 3861–3873.
- (31) Ji, Y.; Wei, Y.; Liu, X.; Wang, J.; Ren, K.; Ji, J. Zwitterionic Polycarboxybetaine Coating Functionalized with REDV Peptide to Improve Selectivity for Endothelial Cells. *J. Biomed. Mater. Res., Part A* **2012**, *100*, 1387–1397.
- (32) Zhang, C.; Yang, H.-C.; Wan, L.-S.; Liang, H.-Q.; Li, H.; Xu, Z.-K. Polydopamine-coated Porous Substrates as A Platform for Mineralized β -FeOOH Nanorods with Photocatalysis under Sunlight. *ACS Appl. Mater. Interfaces* **2015**, *7*, 11567–11574.
- (33) Wang, J.-l.; Ren, K.-f.; Chang, H.; Zhang, S.-m.; Jin, L.-j.; Ji, J. Facile Fabrication of Robust Superhydrophobic Multilayered Film Based on Bioinspired Poly(dopamine)-modified Carbon Nanotubes. *Phys. Chem. Chem. Phys.* **2014**, *16*, 2936–2943.
- (34) Dreyer, D. R.; Miller, D. J.; Freeman, B. D.; Paul, D. R.; Bielawski, C. W. Elucidating the Structure of Poly(dopamine). *Langmuir* **2012**, *28*, 6428–6435.
- (35) Vecchia, N. F. D.; Luchini, A.; Napolitano, A.; D'Errico, G.; Vitiello, G.; Szekely, N.; d'Ischia, M.; Paduano, L. Tris Buffer Modulates Polydopamine Growth, Aggregation, and Paramagnetic Properties. *Langmuir* **2014**, *30*, 9811–9818.
- (36) Mostert, A. B.; Hanson, G. R.; Sarna, T.; Gentle, I. R.; Powell, B. J.; Meredith, P. Hydration-controlled X-band EPR Spectroscopy: A Tool for Unravelling the Complexities of the Solid-state Free Radical in Eumelanin. *J. Phys. Chem. B* **2013**, *117*, 4965–4972.
- (37) Ho, C.-C.; Ding, S.-J. Structure, Properties and Applications of Mussel-inspired Polydopamine. *J. Biomed. Nanotechnol.* **2014**, *10*, 3063–3084.
- (38) Mrówczyński, R.; Markiewicz, R.; Liebscher, J. Chemistry of polydopamine analogues. *Polym. Int.* **2016**, *65*, 1288–1299.
- (39) Wang, J.; Tahir, M. N.; Kappl, M.; Tremel, W.; Metz, N.; Barz, M.; Theato, P.; Butt, H.-J. Influence of Binding-Site Density in Wet Bioadhesion. *Adv. Mater.* **2008**, *20*, 3872–3876.
- (40) Kohri, M.; Kohma, H.; Shinoda, Y.; Yamauchi, M.; Yagai, S.; Kojima, T.; Taniguchi, T.; Kishikawa, K. A Colorless Functional Polydopamine Thin Layer as a Basis for Polymer Capsules. *Polym. Chem.* **2013**, *4*, 2696–2702.
- (41) Shao, Q.; Mi, L.; Han, X.; Bai, T.; Liu, S.; Li, Y.; Jiang, S. Differences in Cationic and Anionic Charge Densities Dictate Zwitterionic Associations and Stimuli Responses. *J. Phys. Chem. B* **2014**, *118*, 6956–6962.
- (42) Luo, R.; Tang, L.; Zhong, S.; Yang, Z.; Wang, J.; Weng, Y.; Tu, Q.; Jiang, C.; Huang, N. In Vitro Investigation of Enhanced Hemocompatibility and Endothelial Cell Proliferation Associated with Quinone-rich Polydopamine Coating. *ACS Appl. Mater. Interfaces* **2013**, *5*, 1704–1714.
- (43) Chen, H.; Zhang, M.; Yang, J.; Zhao, C.; Hu, R.; Chen, Q.; Chang, Y.; Zheng, J. Synthesis and Characterization of Antifouling Poly(N-acryloylaminooxyethanol) with Ultralow Protein Adsorption and Cell Attachment. *Langmuir* **2014**, *30*, 10398–10409.
- (44) Shi, X.; Wang, Y.; Li, D.; Yuan, L.; Zhou, F.; Wang, Y.; Song, B.; Wu, Z.; Chen, H.; Brash, J. L. Cell Adhesion on a POEGMA-modified Topographical Surface. *Langmuir* **2012**, *28*, 17011–17018.